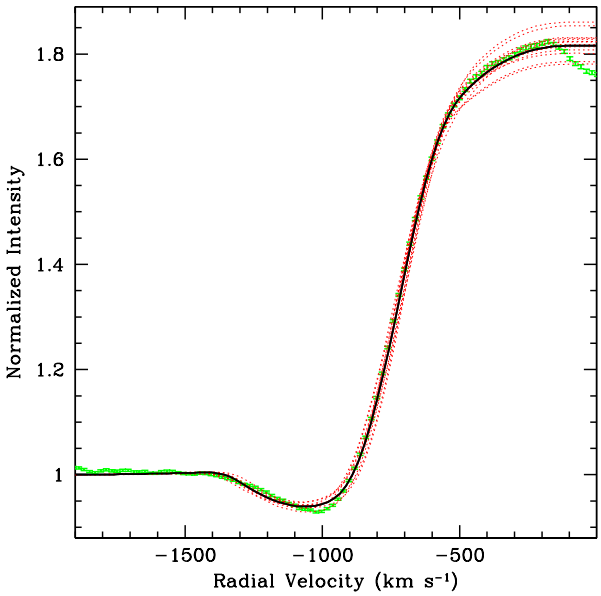

Fig. 7. Effects of changing the input parameters, one by one, on the shape of the line profile. The thick continuous line is the best-fit model. Dotted lines are the models with a different value for one of the following input parameters: $V_{\rm max}$, X_1, X_2, X_3, R_1, R_2, R_3. The observed spectrum (n22) is plotted as individual (green) points with error bars corresponding to S/N∼490. The "dip" in the observed line profile at ∼0 km s^{-1} is the P Cyg absorption component of the neighboring N V 4620 Å line. The color figure can be viewed online.

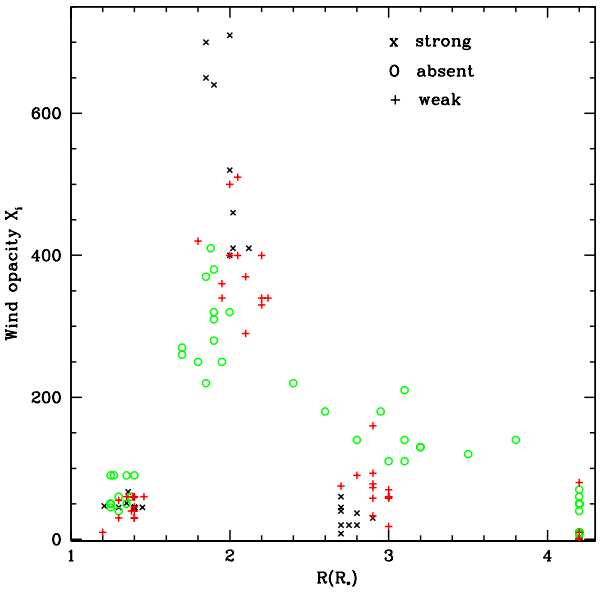

Fig. 8. Opacity parameter values (X_i, i = 1, 2, 3, 4) and their corresponding wind regions(R_i) derived from the line-profile fits. The different symbols indicate the different types of profiles: cross (s), plus sign (w) and circle (a). The color figure can be viewed online.

5. WIND STRUCTURE

Figure 8 shows the plot of the opacity parameter values, X_i, and the corresponding radial extent, R_i, derived from the line fits. The different symbols correspond to the three types of line profiles, *strong*, *weak* and *absent*, which henceforth will be referred to as s, w and a. The first noteworthy feature of this plot is that the opacity is, in general, small within the region closest to the star, ∼1.5 R_*. This is consistent with the NV/NVI $\ll$ 1 abundance ratio in the innermost wind region (Hillier 1988; Figure 2). The opacity then rises significantly in R_2, and then declines again in R_3 and R_4. Thus, the dominant opacity involved in the formation of the N V 4604 line is that of the wind material located in the R_2 region, but with the a profiles having a significant contribution from material in R_3. The second feature is the marked difference in the behavior of the opacity factor in the a profiles from that of the s/w profiles. The former have smaller values of X_2 and larger values of X_3 than the latter.

Given that similar profiles may be obtained with different combinations of $V_{\rm max}$, X_i and R_i, a second set of model fits was computed with $V_{\rm max}$ = const = 40, in order to illustrate the impact on the results. The fits were performed for the s and a profiles, since the w profiles are intermediate between these two. Figure 9 illustrates the difference between the results obtained above leaving $V_{\rm max}$ as a parameter to be fit (left) and holding $V_{\rm max}$ constant (right). The clear separation of the X_i, $i = 1, 2$ values for the s and a profiles persists as does the trend for a larger average value of R_3 in the a profiles.

We now examine the 3.76 d phase dependence of the model fit parameters. In Table 3 we listed the night-to-night sequence of profile types for each epoch of observations. Table 5 shows the same description as Table 3, but the letters s, a, w are here listed in sets of four, corresponding to four consecutive nights of observation (Columns 2–5). In this representation it is evident that for each epoch the profile shape cycles through the type s (day 1), a (day 2) and w/a (days 3 and 4), where w/a means either a w or an a type. Columns 6–10 and 11–14 of Table 5 list the corresponding values of the opacity parameters X_2 and X_3, respectively, in the same representation of sets of four nights. For each epoch, the column corresponding to the s profiles has the largest X_2 value and smallest X_3 value. This table clearly shows the 3.76 d cyclical pattern for